plant biology

Plant Biology ISSN 1435-8603

RESEARCH ARTICLE

Unveiling contrasting iron efficiency strategies in common bean (*Phaseolus vulgaris* L.) genotypes under iron deficiency

F. X. Rucamumihigo[1,2], U. Ludewig[1], A. Hernández-Pridybailo[1,3], I. Cakmak[4] & N. J. Maywald[1]

1 Institute of Crop Sciences, Nutritional Crop Physiology (340h), University of Hohenheim, Stuttgart, Germany
2 Department of Crop Sciences, The University of Rwanda-CAVM, Musanze, Rwanda
3 CIGRAS, Universidad de Costa Rica, San Pedro, Costa Rica
4 Faculty of Engineering & Natural Sciences, Sabanci University, Istanbul, Turkey

Keywords
common bean (*Phaseolus vulgaris*); genotypic variation; Iron efficiency; iron transporters; micronutrient deficiency; plant nutrition.

Correspondence
N. J. Maywald, Institute of Crop Sciences, Nutritional Crop Physiology (340h), University of Hohenheim, 70599 Stuttgart, Germany.
E-mail: niels.maywald@uni-hohenheim.de

Editor
M. Hawkesford

Received: 19 September 2025;
Accepted: 22 April 2026

doi:10.1111/plb.70234

ABSTRACT

- Iron (Fe) deficiency in food crops, particularly on calcareous soils, limits productivity and human nutrition. This study investigated two common bean (*Phaseolus vulgaris*) genotypes, Guaymí (high Fe-accumulating, HI) and Matambú (low Fe-accumulating, LI) to understand physiological and genetic mechanisms underlying Fe uptake, shoot accumulation, and adaptation under low and adequate Fe conditions.
- Plants were grown under controlled Fe-deficient and Fe-sufficient conditions. Root-induced acidification, ferric reductase activity, leaf chlorosis, and Fe and Mn accumulation were measured. Gene expression of Fe-related transporters and mobilisation pathways was assessed at early and prolonged stages of deficiency.
- Under Fe deficiency, HI showed stronger root acidification, higher ferric reductase activity, and greater Fe uptake compared with LI. HI maintained growth, leaf Fe, and Mn content, whereas LI relied on polyphenol-based Fe mobilisation. Early-stage Fe-related gene expression differed between the two genotypes but converged under prolonged deficiency.
- The HI genotype demonstrates superior Fe absorption efficiency and adaptive responses under Fe-limited conditions, sustaining growth and Fe accumulation in roots and shoots. These findings highlight the potential of selecting or engineering Fe-efficient cultivars to improve crop productivity and nutritional quality, offering a promising strategy to address Fe deficiency in agriculture and human diets.

INTRODUCTION

The common bean (*Phaseolus vulgaris*) is one of the most important legumes in the world, accounting for half of all grain legume consumption. It has high commercial and nutritional value, especially in developing countries (Broughton *et al*. 2003; FAO 1999; Rawal 2019). Bean seeds contain higher amounts of iron (Fe) and zinc (Zn) than cereals, rendering them a strategic crop for addressing micronutrient deficiencies in the human diet (Welch & Graham 2004). Globally, approximately 5 billion and 3.5 billion people consume inadequate amounts of Fe and Zn in their diets, respectively (Passarelli *et al*. 2024). This micronutrient scarcity mainly affects children and women of reproductive age (Ritchie & Roser 2019; Stevens *et al*. 2022). In East and Central Africa, where beans are a staple food, Fe intake is minimal, and alternative sources of Fe are often culturally unacceptable or unaffordable (Broughton *et al*. 2003; Passarelli *et al*. 2024).

Although selecting cultivars with high bean seed Fe accumulation has the potential for improving Fe delivery (Bouis & Saltzman 2017), seed Fe concentration alone does not guarantee bioavailability (Glahn & Noh 2021). Iron bioavailability is strongly affected by anti-nutritional factors in seeds, including polyphenols, phytate, tannins, and resistant cell walls, which can reduce Fe absorption in both humans and animals (Petry *et al*. 2015; Glahn *et al*. 2016; Hart *et al*. 2017, 2020). While nutritional enhancement remains a long-term breeding goal, seed Fe accumulation can provide valuable insights into a plant's efficiency in Fe uptake, transport, and homeostasis.

The ability of plants to accumulate Fe in seeds may reflect their enhanced Fe acquisition and internal distribution capacity, particularly in Fe-limited soils. Genotypic variation in Fe uptake and accumulation can optimise plant Fe nutrition, as demonstrated in other Fabaceae, such as soybean, where Fe and Zn accumulation QTLs co-localise with loci conferring tolerance to iron deficiency chlorosis (King *et al*. 2013). In chickpea, genotype-specific transcriptomic and metabolite responses under Fe deficiency reflect differences in both stress tolerance and nutrient accumulation (Singh *et al*. 2023a). In peanuts, higher seed Fe content, together with the accumulation of resveratrol and ferulic acid, has been linked to improved performance in calcareous soils (Singh *et al*. 2023b). These findings suggest that seed Fe accumulation may serve as a physiological marker for efficient Fe homeostasis under limiting conditions.

Although cultivated soils are rich in total Fe, it is often not phytoavailable and poorly soluble for root uptake, mainly because of a high soil pH (Schulte 2004; Broadley *et al*. 2012). Today, many arable areas have calcareous soils, resulting in low plant Fe and low crop production (Rodríguez-Lucena *et al*. 2010; Shukla *et al*. 2021). Plants in such Fe-deficient soils often develop characteristic 'lime-induced chlorosis' (FAO 2015).

In dicots such as the common bean, Fe acquisition follows Strategy I mechanisms (Römheld & Marschner 1986), which involve rhizosphere acidification through the release of protons mediated by root H^{+}- ATPase activity (Santi & Schmidt 2009). In addition, Fe^{3+} chelates are then reduced to Fe^{2+} via electron transfer across the root cell membrane by ferric chelate reductase oxidase (FeCR) activity, which is encoded by the ferric reductase oxidase (*FRO*) gene family (Chaney *et al.* 1972; Robinson *et al.* 1999; Connolly *et al.* 2003). Fe^{2+} is then transported into root cells by the iron transporter *IRT1*, a member of the zinc/iron-regulated transporter-like protein (ZIP) family. This family includes additional genes, such as *ZIP1* and *ZIP2*, which also regulate Zn uptake (Bereczky *et al.* 2003; Lin *et al.* 2009). Strategy I plants can also secrete phenolic compounds into the rhizosphere to complex and mobilise Fe, thereby enhancing Fe uptake (Rodriguez-Celma *et al.* 2013). For further transport through the xylem or phloem, Fe^{2+}/Fe^{3+} is chelated by citric acid and nicotianamine, the latter of which is synthesised by the *NAS1* and *NAS2* genes (von Wirén *et al.* 1999; Durrett *et al.* 2007; Schuler *et al.* 2012). Fe accumulation and storage occur via the heme protein ferritin, encoded by the *FER1* gene, which also sequesters excess iron and protects the plant from iron toxicity (Roschzttardtz *et al.* 2013). However, in common bean seeds, ferritin accounts for only a small proportion of Fe (15–29%), and most of this (70–85%) is in the non-ferritin-bound form, which is thought to be phytate (Hoppler *et al.* 2009). High Fe-accumulating varieties often show an increased capacity to release H^{+} ions, reduce Fe^{3+} to Fe^{2+}, and release organic acids (Brown 1972). These traits contribute to the translocation and redistribution of Fe in shoot plant organs and higher grain Fe content (Wiersma 2012; Santos *et al.* 2015).

However, high Fe accumulation is occasionally associated with undesirable plant growth and metabolic trade-offs. For example, high Fe is associated with reduced seed sink strength, as evidenced by fewer poorly filled pods and lower yield, which can misleadingly inflate Fe content owing to smaller seed mass (Beebe 2020). Finally, high Fe levels interact with other plant nutrients: positive correlations with Zn, S, Mn, and P (Beebe *et al.* 2000), positive correlations with Zn and Cu, and a negative correlation with Mn have also been reported (Moraghan *et al.* 2002; Wiersma 2005; Ghandilyan *et al.* 2006; Pinheiro *et al.* 2010).

This study sought to explore how variations in Fe content across common bean genotypes modulate key metabolic pathways and interact with other micronutrients, such as Zn and Mn, under iron deficiency. We hypothesise that differences in seed Fe content between genotypes may influence the regulation of metabolic pathways involved in nutrient uptake and stress responses, particularly under Fe-limiting conditions. Specifically, we aim to determine if the coordination of Fe-related traits (e.g., Fe uptake, root acidification, and ferric reduction) is governed by genetic mechanisms, such as the upregulation of genes linked to Fe acquisition and secondary metabolism, and whether this regulation differs between high- and low-efficiency genotypes.

To test this hypothesis, two common bean genotypes were selected from a pool of 25, characterised by low- and high-seed Fe concentrations. This study will focus on examining growth medium acidification, ferric reductase activity, shoot Fe accumulation, and the expression of Fe-related genes under Fe deficiency. Here, we evaluate whether differences in Fe concentration between these genotypes are associated with traits of Fe efficiency by analysing physiological and molecular responses.

MATERIALS AND METHODS

Plant material

A total of 25 *Phaseolus vulgaris* genotypes were screened for seed Fe, Zn, and Mn concentrations, including 19 genotypes from Rwanda (Rwanda Agricultural Board) and six genotypes from Costa Rica (Estación Experimental Agrícola Fabio Baudrit Moreno, Universidad de Costa Rica). Seeds used for mineral analysis were produced within each region during the same cultivation cycle and under uniform field conditions, ensuring comparable growing conditions within each group of genotypes. Two common bean genotypes with the same origin, similar yield and phenology, seed coat colour (black), morphology, and phytic acid (PA), total phosphorus (P), and total polyphenol content but contrasting grain Fe, Zn, and Mn concentrations were chosen for further analysis (Table 1). The genotype Guaymí, with a high concentration of Fe in the seed, was named 'High-seed-Iron-accumulating (HI, 75.0 mg Fe kg^{-1} seed).' In contrast, the genotype Matambú was the one with low Fe and was named 'Low-seed-Iron-accumulating (LI, 52.6 mg Fe kg^{-1} seed).' Methods for the quantification of Fe, Zn, Mn, P, PA, and total polyphenols are described in detail in the corresponding sections below.

Table 1. Performance and composition in grains of the two studied genotypes; Guaymí (high seed iron-accumulating, HI) and Matambú (low seed iron-accumulating, LI) 100-seed weight, yield, phytic acid (PA), total phosphorus (P), total polyphenols, Fe, Zn, and Mn grain concentrations.

	genotypes		signif. (*t*-test HI vs. LI)
	Guaymí (HI)	Matambú (LI)	
100-seed weight (g)	19.1 ± 1.5	19.9 ± 1.8	ns
Yield (kg ha^{-1})[a]	1264 ± 425	1376 ± 353	ns
Phytic acid (mg g^{-1})	19.3 ± 3.8	17.5 ± 2	ns
Total P (mg g^{-1})	5.44 ± 1	4.94 ± 0.5	ns
Total polyphenols (mg g^{-1})	10 ± 3.4	13 ± 3.6	ns
Fe (mg kg^{-1} seed DM)	74.88 ± 6.1	52.57 ± 0.9	*
Zn (mg kg^{-1} seed DM)	37.00 ± 1.09	26.69 ± 0.51	***
Mn (mg kg^{-1} seed DM)	22.7 ± 0.7	12.8 ± 0.07	**

The means and SD (n = 6 for Fe, Zn, and Mn; n = 13 and 11 for yield of LI and HI, respectively, and n = 10 for 100-seed weight of both genotypes, n = 6 for P and PA) of the two genotypes were compared using an independent *t*-test.

DM = dry matter; GAE = gallic acid equivalents; ns = non-significant.

[a] Mean across various Costa Rican regions from 2003 to 2012.

*$P < 0.05$.

**$P < 0.01$.

***$P < 0.001$.

Determination of Total phosphorus (P) and Phytic acid (PA)

Total P and PA were measured using a PA and total phosphorus assay kit (K-PHYT, Megazyme, Bray, Ireland) following the manufacturer's instructions. With this kit, basically, PA of 1 g of ground seed material was extracted with 20 ml of 0.66 M hydrochloric acid, then followed a series of dephosphorylations with phytase and phosphatases (all come with the kit); the phosphate released from PA was measured using a modified colorimetric molybdenum blue assay at 655 nm and calculated as total P and PA content of the original sample.

Seed germination and growing conditions

For seed surface sterilisation, 20 g of seeds were immersed in 10% H_2O_2 mixed with 1 ml surfactant (Tween 20) and shaken for 10 min at 200 rpm on an orbital shaker (SM 30; Edmund Bühler GmbH, Bodelshausen, Germany). The seeds were then washed three times with running distilled water. For germination, seeds were rolled in filter paper and placed vertically in a solution of 3 mM $CaSO_4$ for 5 days in the dark at 25°C. Germinated seedlings were transferred individually to 1-L tulip glass jars (SKU: F745; Weck, Bonn, Germany) covered with aluminium foil. The jars contained a continuously aerated nutrient solution with the following composition (mM): $Ca(NO_3)_2.\ 4H_2O$, 2; KH_2PO_4, 0.1; K_2SO_4, 0.7; $MgSO_4.7H_2O$, 0.5; KCl, 2.7; $ZnSO_4.7H_2O$, 0.5; $CuSO_4.5H_2O$, 0.2; H_3BO_3, 1.7; $MnSO_4.H_2O$, 0.5; $NH_4Mo_7O_{24}.4H_2O$, 0.01 with or without 45 µM Fe (III)ETDA. The pH of the nutrient solution was adjusted to 6.0 with 1 M KOH. Plants were grown at 25°C–20°C (day and night temperatures respectively), 70% relative humidity, under a 16/8 h light/dark regime, and at a photosynthetic photon flux density of 300 $\mu mol\ m^{-2}\ s^{-1}$. The nutrient solution was regularly changed every 3 days, and plants were harvested 10 days after being transferred into the growth chamber. Cotyledons were removed after unifoliate leaves were unfurled on the second day of transfer to the growth chamber.

Growth and morphological parameters

The chlorophyll content of the leaves was estimated by soil and plant analyser development (SPAD) readings using a portable chlorophyll meter (SPAD-502Plus; Konica Minolta Sensing, Inc., Osaka, Japan). SPAD readings were taken from both the primary leaves and the fully expanded apical trifoliate leaf. For primary leaves, four technical replicates were recorded per leaf, and their average was used for each plant. For the apical trifoliate, one SPAD measurement was taken from each of the three leaflets, and their average represented the value per plant. The roots and shoots were separately sampled, rinsed with distilled water, and dried at 70°C for 48 h. The dried samples were ground and microwave-digested to measure micronutrients using atomic absorption spectrometry (AAS).

Root acidification capacity

The acidification capacity of the plants was measured daily by monitoring pH changes in the growth media. To assess the ability of the plants to release protons into the growth medium and to isolate fluctuations in pH as the plants adapted to the fresh nutrient media (every 3 days, the medium was changed), acidification was additionally measured on Day 8. Day 8 was chosen because it corresponded with the lowest pH values in the iron-starved plants. Roots of intact plants were placed in fresh glass jars containing 200 ml of continuously aerated solution. The solution comprised 10 mM KCl and 1 mM $CaCl_2{\cdot}2H_2O$ adjusted to a pH of 6.0 with 1 M KOH. The plants remained in the solution for 6 h, and pH readings were recorded every 30 min using a portable pH meter (Fisherbrand Hydrus 300, Fisher Scientific).

Root-based FeEDTA reduction

The reduction of FeEDTA by plant roots was measured according to the methods of Chaney *et al.* (1972) and Vasconcelos *et al.* (2006), with some minor modifications. Intact roots of each plant were submerged in a 100 ml solution containing 0.5 mM $CaSO_4.2H_2O$, 0.1 mM EDTA, 0.3 mM bathophenanthrolinedisulfonic acid (BPDS), and 10 mM 2-N-morpholine ethane sulfonic (MES) adjusted to pH 5.5 with 1 M KOH. The absorbance of Fe^{2+}chelated to BPDS was measured at 535 nm on a molar extinction coefficient of 22 nm cm^{-1}. An aliquot of the solution without roots was used as a blank. The assay was conducted under dim light conditions for 45 min. All plants used in the root-based iron reduction assay were discarded and not used for further analysis.

Total phenolic and flavonoid content determination

The concentration of total polyphenols in seeds was measured using the method of Ainsworth & Gillespie (2007). For this purpose, 20 mg of finely ground seed dry mass was mixed with 2 ml of ice-cold 95% methanol (v: v). The mixture was incubated in the dark at room temperature for 48 h and then centrifuged at 13000 × *g* for 5 min. The supernatant (100 µL) was mixed with 200 µl of 10% Folin and Ciocalteu (F-C) phenol reagent and 800 µl of 700 mM Na_2CO_3. The mixture was incubated for 2 h, and the absorbance was measured spectrophotometrically at 765 nm using a FLUOstar Omega microplate reader (BMG Labtech, Ortenberg, Germany). A standard curve from 0 to 1 mM gallic acid (Sigma-Aldrich, St. Louis, United States) was used to determine total phenolics as gallic acid equivalents (GAE). The concentrations of total polyphenols and total flavonoids in roots and leaves were determined following the method of Bravo-Monzón *et al.* (Bravo-Monzón *et al.* 2022) with minor modifications. For total polyphenols, 50 mg of frozen ground tissue was extracted and incubated as described above for seed samples. The supernatant (40 µl) was mixed with 960 µl of methanol (95%), vortexed and then mixed with 200 µl of the F-C reagent, vortexed again. After 30 min of incubation, 800 µl of Na_2CO_3 (700 mM) was added, the mixture was covered and incubated for 2 h after which it was centrifuged at 13000 × *g*, then the absorbance was measured at 735 nm. The standard curve from 0 to 200 mg L^{-1} gallic acid (Sigma-Aldrich, St. Louis, United States) was used to determine total phenolics as GAE. For total flavonoids, the supernatant (20 µl) was mixed with 80 µl of deionised water, followed by the addition of 30 µl of 5% $NaNO_2$ and incubation for 5 min. Subsequently, 30 µl of 10% $AlCl_3$ was added and the mixture was incubated for 1 min. The reaction was then neutralised with 200 µl 1 M NaOH and adjusted to a final volume of 1 mL by adding 640 μl of deionised water. The final mixture was vortexed for 10 s, and 300 μl was removed for measuring the absorbance at 510 nm. A standard curve generated from a range of 0–200 mg L^{-1} mM catechin (Sigma-Aldrich, St. Louis, United States) was used to determine total flavonoids as catechin equivalents.

RNA extraction, quantification and cDNA synthesis

In a parallel experiment, additional plants were cultivated under the same growth conditions described above to analyse the molecular responses of iron-dependent genes. Frozen root and leaf (primary leaf) samples from five plants (biological replicates) were meticulously ground into a fine powder using a mortar and pestle. Total RNA was extracted using a modified cetyltrimethylammonium bromide (CTAB) method following Murray & Thompson (1980) and Gambino *et al.* (2008). Ultrapure water not treated with DEPC was used to prepare all the solutions. The extraction buffer contained 4% CTAB, 25 mM EDTA, 2 M NaCl, 100 mM Tris–HCl (pH 8), 0.5 g L^{-1} spermidine, 25 μM DTT, and 4% 2-mercaptoethanol. The pH of the extraction buffer was adjusted to 8. Additional reagents included 0.5% SDS (w/v), 10 M LiCl, chloroform alcohol (24:1 v/v), 75% ethanol, and 4% 3 M NaAc in absolute ethanol. Except for ethanol and chloroform, all solutions were incubated overnight at 37°C and autoclaved twice for 20 min at 121 °C. RNA quality and quantity were assessed using a NanoDrop 2000c Spectrophotometer (Thermo Fisher Scientific Inc., Waltham, United States) for UV spectrophotometry measurements. Genomic DNA removal and cDNA synthesis were performed using the QuantiTect Reverse Transcription Kit (Qiagen, Venlo, Netherlands) according to the manufacturer's instructions.

Relative quantification of gene expression by qRT-PCR

Gene expression analysis was conducted for six target genes: *PvIRT1* (*P. vulgaris Iron-Regulated Transporter 1*), *PvFER1* (*P. vulgaris Ferritin 1*), *PvFRO1* (*P. vulgaris Ferric Reductase Oxidase 1*), *PvNAS1* (*P. vulgaris Nicotianamine Synthase 1*), *PvNAS2* (*P. vulgaris Nicotianamine Synthase 2*), and *PvZIP2* (*P. vulgaris Zinc/Iron-Regulated Transporter-Like Protein 2*), as detailed in Table S1. Actin and Tubulin were used as internal controls to normalise all qRT-PCR reactions. *PvNAS1* is predicted to be *P. vulgaris* nicotianamine synthase (LOC137814907), while *PvNAS2* is predicted to be *P. vulgaris* nicotianamine synthase-like (LOC137831934). These genes were selected based on their significant roles in transport and accumulation, in alignment with the Strategy I mechanism described for dicot plants (Urwat *et al.* 2021). qRT-PCR reactions were conducted on a CFX384 Real-time system (Bio-Rad Laboratories, Hercules, CA, USA). The reaction conditions were as follows: 20 min at 95°C, followed by 49 cycles of 30 s at 95°C, 60 s at 60°C, and 31 s at 65°C. Amplifications were performed using 0.3 μL of specific primers (diluted 1:100), mixed with 7.5 μL of 2× Green Master Mix FAST without ROX for qPCR (GENAXXON Bioscience GmbH, Ulm, Germany) and 5 μL of cDNA (3 ng μL^{-1}), with a final reaction volume of 15 μL. Each gene (and the controls) was tested in five biological replicates, considering three technical replicates for qPCR. Melt curve profiles were analysed for each gene to confirm the specificity of amplification. Gene expression data for the target genes were normalised to those of the control genes. Expression data for selected genes (*IRT1, FER1, FRO1, NAS1, NAS2, ZIP2*) were filtered, log-transformed (log1p), and scaled using min–max normalisation to highlight relative expression differences across samples. Scaled normalised expression was visualised using R (version 4.3.1, 2023-06-16), with the following packages: tidyverse (version 2.0.0), magrittr (version 2.0.3), pheatmap (version 1.0.12), dplyr (version 1.1.4), and tidyr (version 1.3.1).

Total Fe, Zn and Mn determination by atomic absorption spectrometry (AAS)

Roots, trifoliate leaves, and the remaining shoot tissues (stems and unifoliate leaves) from the two bean genotypes were dried and ground prior to analysis. The samples were then ashed in a furnace at 500°C for 4 h, cooled, and wetted with a few drops of deionised water, and then ashed again for 1 h. After cooling, the combined ash residue was evaporated with 1:3 HNO_3 on a heating plate to remove SiO_2 and then dissolved in 1:3 HCl. The final clear solution was diluted to the final volume with deionised water and analysed with an atomic absorption spectrophotometer (iCE3300 AAS, ThermoFisher Scientific, Karlsruhe, Germany).

Statistical analysis

Statistical analyses were performed using R version 4.3.1 (2023-06-16) and RStudio Version 2023.06.2 + 561 (2023-08-25). Data are presented as mean ± standard deviation (SD) unless otherwise stated. Normality and homogeneity of variance were assessed using the Shapiro–Wilk test and Levene's test, respectively, and visually examined with QQ-plots, histograms, and residual plots. Comparisons between two groups were performed using independent or paired *t*-tests as appropriate. Statistically significant differences were indicated using asterisks: $* = P \leq 0.05$, $** = P \leq 0.01$, $*** = P \leq 0.001$. When the assumptions of the *t*-test were not met, a non-parametric alternative (Mann–Whitney *U* test or Wilcoxon signed-rank test) was applied.

RESULTS

Screening of seeds from 25 *P. vulgaris* genotypes for micronutrient concentrations of Fe, Zn, and Mn revealed clear and significant differences. The lowest Fe concentrations were observed in seeds from genotype rw_bb_183_b with 51.94 ± 5.16 mg kg^{-1} dry matter (DM), closely followed by Matambú with 52.57 ± 0.99 mg kg^{-1} DM (Table 1). In contrast, the highest Fe concentrations were observed in genotype RWV_3316 (75.31 ± 3.47 mg kg^{-1} DM) and in Guaymí, which showed similarly high levels (74.99 ± 6.15 mg kg^{-1} DM). For further analysis, Matambú and Guaymí were selected and named LI and HI, based on their high and low Fe-accumulating capacity in the seed. Furthermore, the two genotypes with contrasting seed Fe storage capacities differed widely in their Zn and Mn concentrations. Based on the micronutrient concentrations (Fig. 1), LI and HI were also identified as the most contrasting candidates. LI seeds contained 26.69 ± 0.51 mg kg^{-1} DM of Zn and 12.85 ± 0.07 mg kg^{-1} DM of Mn, while HI seeds exhibited higher concentrations, with 37.00 ± 1.09 mg kg^{-1} DM of Zn

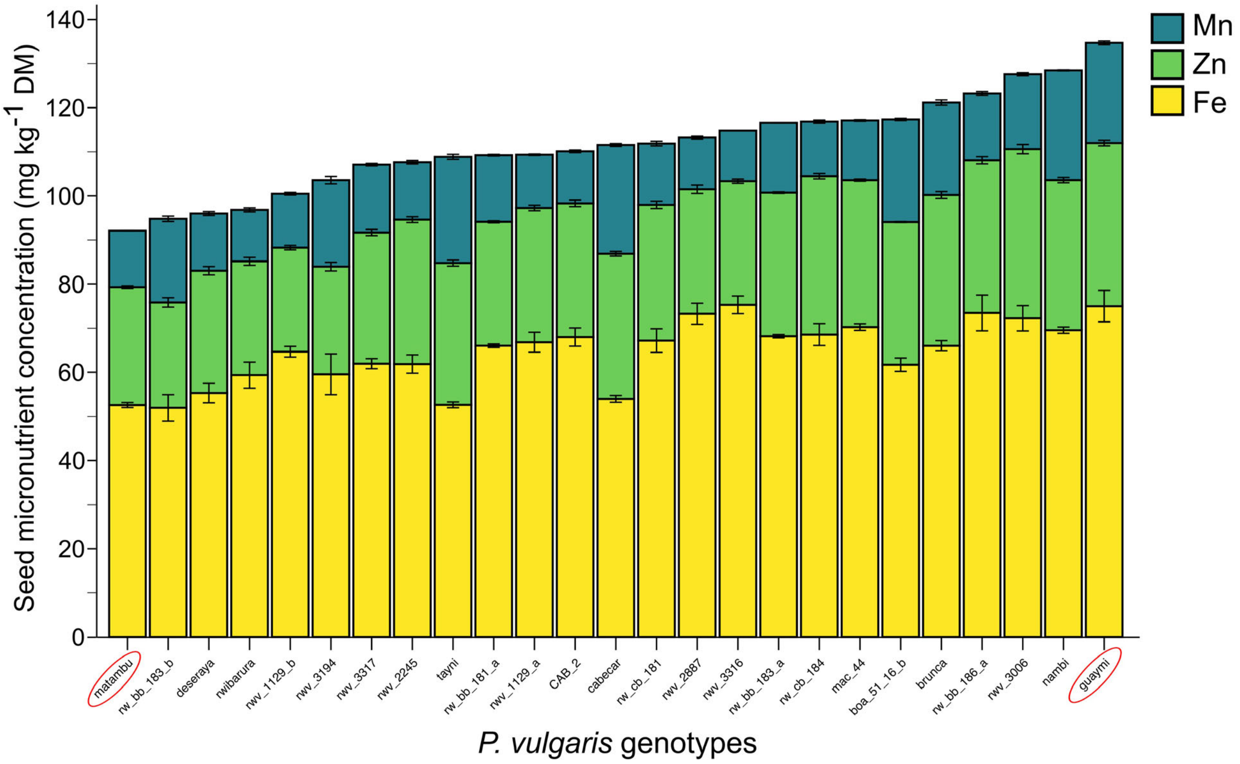

Fig. 1. Seed micronutrient concentrations of Fe, Zn, Mn (mg kg^{-1} DM). Seeds from 25 different common bean (*P. vulgaris*) genotypes from Rwanda and Costa Rica. Data represent means ± SD of three biological replicates.

and 22.70 ± 0.72 mg kg^{-1} DM of Mn. These two genotypes were considered suitable for comparative analysis because of their root morphology and semi-determinate growth habit similarities (type II b). Additionally, both genotypes show similar yield, 100-seed weight, and black seed coat. They also belong to the same market class. Moreover, because total P, PA, and total polyphenol seed concentrations affect micronutrient interactions and Fe bioavailability (Glahn & Noh 2021), these parameters were evaluated. They were found to be similar (Table 1). A previous report confirmed no differences in total seed polyphenol concentrations between HI (Guaymí) and LI (Matambú) (León-Cortés *et al.* 2025). This is consistent with the present observations. Therefore, the studied genotypes fulfilled the conditions of contrasting primarily in micronutrient concentration while being similar in almost all other aspects. This eliminates bias and ensures a reliable comparison between 'High' and 'Low'-Fe genotypes.

Growth responses and chlorophyll status under Fe deficiency

After 10 days of growth, the root and shoot dry weights indicated that the total plant dry weight decreased in both genotypes under Fe-deficient conditions (Fig. 2A). Under these conditions, HI exhibited a more pronounced reduction in growth than LI, with dry weights reduced by 20.40% and 31.62%, respectively.

SPAD values, which indicate chlorophyll concentration and leaf chlorosis, showed no difference in primary leaves between HI and LI in both iron treatments (Fig. 2B). However, LI exhibited reduced SPAD values in primary and apex leaves. Under Fe deficiency, both genotypes showed substantial reductions in SPAD values in apex leaves, with HI (19.2 ± 1.48) maintaining higher values than LI (11.38 ± 0.32). Pictures of both genotypes showing the visual symptoms of iron deficiency are shown in Fig. 2C.

Genotypic variations in iron uptake efficiency

The media pH was initially set to 6.0 on day one, with daily pH measurements starting on day three. These daily records showed fluctuations but generally trended toward increased acidity. Overall, pH decreased from an average of 6.64 ± 0.01 on Day 3 to 5.66 ± 0.04 on Day 8 (Fig. 3A). Under Fe-sufficient conditions, pH levels remained consistent across genotypes. However, Fe deficiency led to more significant media acidification, with genotypes responding differently: HI maintained a more acidic medium than LI, with notable differences on Days 4, 5, and 8. For example, HI's pH on day eight was 4.72 ± 0.13, compared with 5.88 ± 0.04 for LI. Significant genotypic, iron-dependent, and interactive effects were observed ($P < 0.001$).

To assess acidification capacity independently of media solution changes, proton extrusion was measured in a medium containing only KCl and $CaCl_2$, adjusted to a pH of 6.0. Under Fe-sufficient conditions, both genotypes displayed similar pH plateaus (Fig. 3B). In contrast, under Fe deficiency, the growth medium of HI exhibited a markedly lower pH (average 4.46 ± 0.17) compared with that of LI (average 5.22 ± 0.13) from 2 to 6 h into the experiment (Fig. 3B), with HI's pH averaging 14.6% lower than LI's.

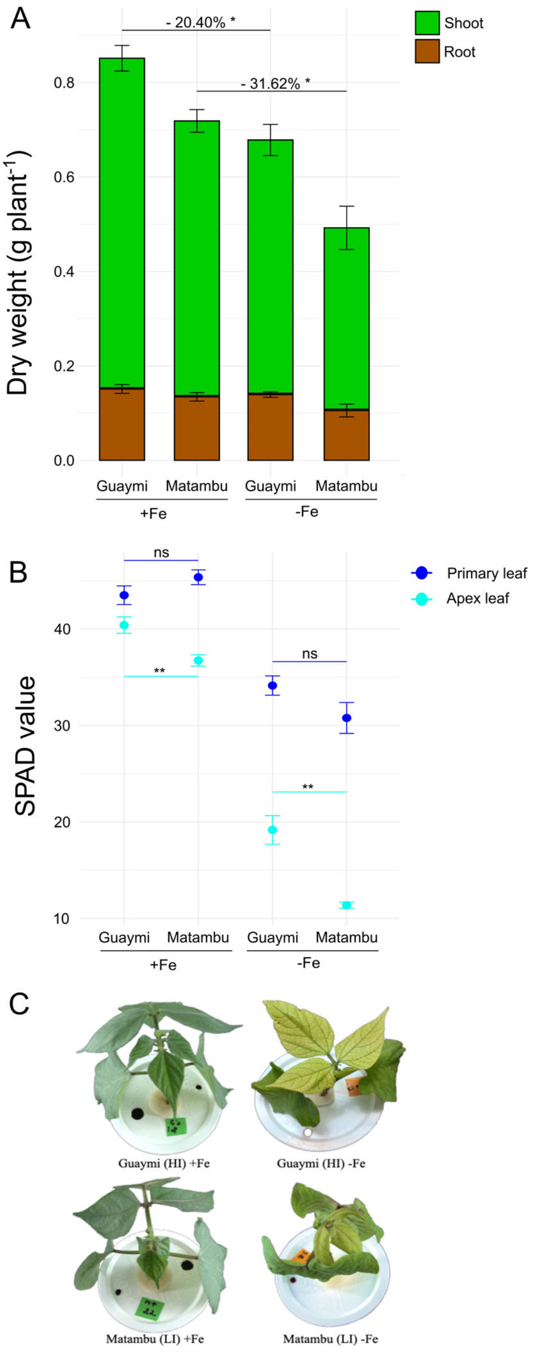

Guaymi (HI) +Fe Guaymi (HI) -Fe

Matambu (LI) +Fe Matambu (LI) -Fe

Fig. 2. (A) Plant growth quantified by dry weight and (B) chlorosis assessment using SPAD values measured on primary leaves and the apex trifoliate leaf in two Phaseolus vulgaris genotypes: Guaymí (HI) and Matambú (LI). Plants were grown hydroponically under sufficient (+Fe, 45 µM FeEDTA) and deficient (-Fe, 0 µM FeEDTA) Fe conditions. Data represent means ± SD of five biological replicates. (C) Images of the plants: HI (top) and LI (bottom) plants after 10 days of growth under iron-sufficient conditions (left) and iron deficiency conditions (right). (A) Independent *t*-tests were performed within each variety to compare treatments. (B) Differences between in SPAD values between varieties within each compartment (primary or apex leaf) and iron treatment were assessed using paired *t*-tests. Asterisks indicate statistically significant differences between iron treatments; * = $P \leq 0.05$; ** = $P \leq 0.01$).

Iron deficiency also increased polyphenol secretion in both the leaves and roots of bean genotypes, with notable genotypic differences (Fig. 4A). Under Fe deficiency, LI produced higher total polyphenols in leaves (280 ± 60 mg g^{-1} FW) compared with HI (197 ± 30 mg g^{-1} FW). A similar but less pronounced trend was observed in roots, where LI produced 201 ± 61 mg g^{-1} FW compared with HI's 177 ± 31 mg g^{-1} FW, yielding 1.4- and 1.1-fold higher polyphenols than HI in leaves and roots, respectively. At the same time, under Fe-sufficient conditions, root polyphenols were reduced in LI compared with HI.

Flavonoid concentrations differed significantly between genotypes in leaves but not in roots, at both Fe supply levels. Under Fe sufficiency, LI showed the highest total flavonoid concentrations in leaves (43 ± 7 mg g^{-1} FW) compared with HI (34 ± 3.4 mg g^{-1} FW), translating to 1.2 more flavonoids of LI when compared with HI (Fig. 4B).

Root FeCR activity, assessed under Fe-sufficient and Fe-deficient conditions, was higher in HI under Fe deficiency, with HI reducing iron to a greater extent (2.39 ± 0.19 µmol Fe^{2+} g^{-1} root FW) than LI (1.09 ± 0.13 µmol Fe^{2+} g^{-1} root FW) (Fig. 4C). In this condition, HI's FeCR activity was 54.4% higher than that of LI.

Micronutrient partitioning and genotypic responses to Fe deficiency

The partitioning of selected micronutrients (Fe, Zn, and Mn) was measured in the roots, shoots, and apex trifoliate of the two bean genotypes grown under Fe-sufficient and Fe-deficient conditions. As expected, Fe content, consistent with its low mobility, was highest in the roots and decreased in the above-ground organs. Under Fe-sufficient conditions, the Fe content in the root and apex trifoliate was similar between the genotypes (Fig. 5A), with the only difference observed in the shoot, where LI exhibited a lower Fe content than HI.

Under Fe deficiency, genotypic differences in the Fe content were pronounced. HI retained a significantly higher Fe content in the root (7.51 ± 1.13 µg plant^{-1}) than LI (1.41 ± 0.25 µg plant^{-1}), representing a 6.6-fold increase in HI. There was no difference in shoot and apex trifoliate Fe content between genotypes under Fe deficiency.

The Zn content followed a trend similar to that of Fe, with the highest levels in the root and the lowest in the apex trifoliate. Root Zn levels were similar across genotypes and Fe conditions. HI accumulated higher Zn levels in the shoots than LI under both Fe conditions (Fig. 5B). In the apex trifoliate under Fe deficiency, HI (3.02 ± 0.54 µg plant^{-1}) maintained higher Zn than LI (1.11 ± 0.286 µg plant^{-1}).

There was no difference in root Mn content between genotypes under either Fe condition (Fig. 5C). However, Fe deficiency led to increased Mn accumulation in the shoots of both genotypes. Under Fe sufficiency, HI accumulated more Mn in the shoots than LI. In the apex trifoliate under Fe deficiency, Mn content was significantly higher in HI (7.90 ± 1.90 µg plant^{-1}) than in LI (2.30 ± 0.40 µg plant^{-1}), with HI exhibiting a 3.4-fold increase in Mn content relative to LI.

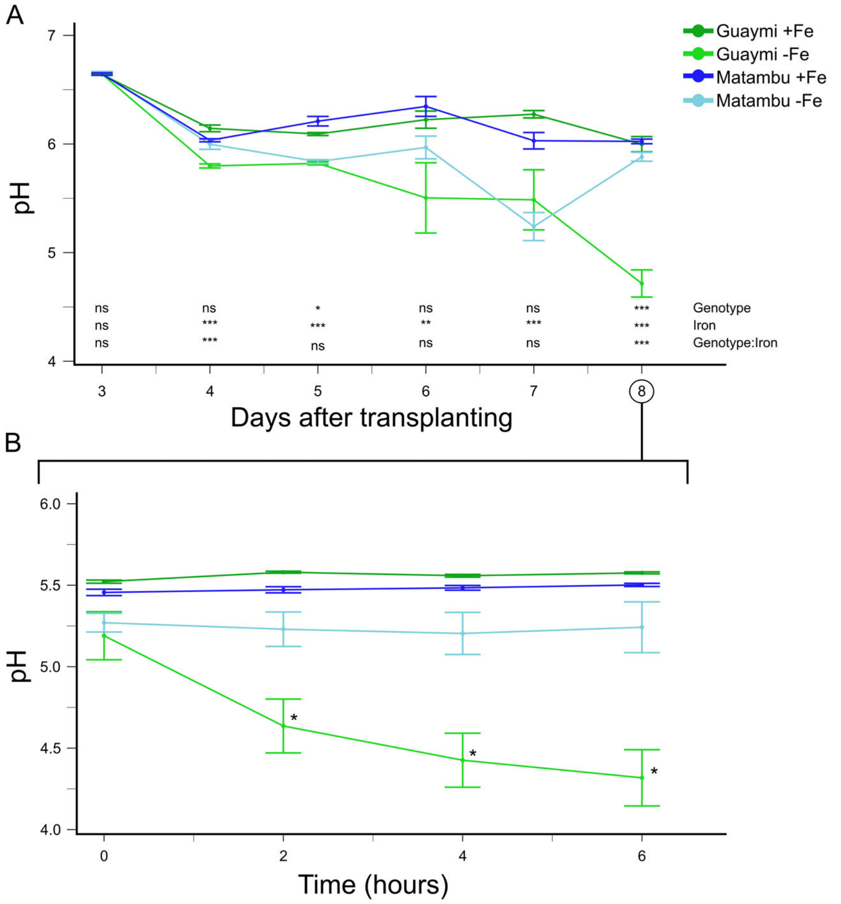

Fig. 3. (A) Acidification of the growth medium (3–8 days after transplanting) was monitored in two common bean genotypes, Guaymí (HI) and Matambú (LI), grown hydroponically under sufficient (+Fe, 45 μM FeEDTA) and deficient (-Fe, 0 μM FeEDTA) Fe conditions. (B) The acidification capacity was additionally assessed by transferring plants after 8 days in a medium containing 10 mM KCl and 1 mM $CaCl_2$. Data represent means ± SD of five biological replicates. (A) Statistical analysis was conducted using ANOVA followed by Tukey's test at $P \leq 0.05$; ns = not significant; ns = not significant; * = $P \leq 0.05$; ** = $P \leq 0.01$; *** = $P \leq 0.001$. (B) For each variety and time point, differences between iron treatments were assessed using two-sample Student's *t*-tests ($P < 0.05$), with *P*-values adjusted using the Bonferroni method.

Genotypic and tissue-specific responses of iron-responsive genes under variable iron conditions

The expression levels of six iron-responsive genes, *IRT1, FER1, FRO1, NAS1, NAS2*, and *ZIP2*, in root and leaf tissues were measured in the two bean genotypes, HI and LI, across multiple iron conditions: Fe sufficiency (+Fe), Fe deficiency (−Fe), Fe resupply (1- and 4-h post-resupply), and Fe deficiency (4-, 24-, and 72-h post-removal) (Fig. 6).

In root tissues under Fe-sufficient conditions, both genotypes displayed relatively low expression levels across all genes, with enhanced expression of *FRO1* and *NAS1* in HI plants and *NAS1* in LI plants. When exposed to prolonged Fe deficiency, both HI and LI roots showed similar upregulation of *IRT1, NAS1*, and *NAS2*, indicating comparable responses to low Fe levels across genotypes. Differences emerged following the Fe resupply. In HI roots, *IRT1* and *NAS1* expression increased within the first hour and intensified after 4 h. *NAS2* and *FER1* exhibited enhanced expression at the 4-h mark, suggesting HI's dynamic response to iron reintroduction. In contrast, LI roots exhibited only moderate upregulation of *IRT1, NAS1*, and *NAS2* at 1 and 4 h, indicating a less robust response. Within the first few hours of Fe deficiency, HI roots showed a sustained increase in *IRT1* expression, peaking at 72 h, indicating a prolonged adaptive response. *NAS1* also remained elevated throughout the duration, while *FRO1* and *FER1* peaked at 24 h, reflecting HI's steady acclimation to iron deprivation. In LI roots, *IRT1* showed minimal change under Fe deficiency, while *FER1, FRO1, NAS1, NAS2*, and *ZIP2* were sharply upregulated at 4 h and subsequently decreased. *FER1* expression was reduced by 24 h, while NAS1 showed a distinctive dip at 24 h, followed by a secondary rise at 72 h. These observations suggest that LI responds to Fe depletion more transiently than HI.

In leaf tissues, both genotypes generally exhibited lower gene expression than roots across all conditions, suggesting that leaf responses to iron fluctuations were subdued relative to roots. Under Fe-sufficient conditions, HI leaves displayed strong upregulation of *FER1*, whereas LI leaves showed moderate *FER1* expression. Upon Fe deficiency, HI leaves upregulated *FER1* within 4 h, with levels tapering off gradually over time. Additionally, *FRO1* exhibited mild upregulation at 24 h, and *NAS1* showed consistent, mild upregulation across all time points. In LI, *FER1* increased at 4 and 24 h, while *NAS1*

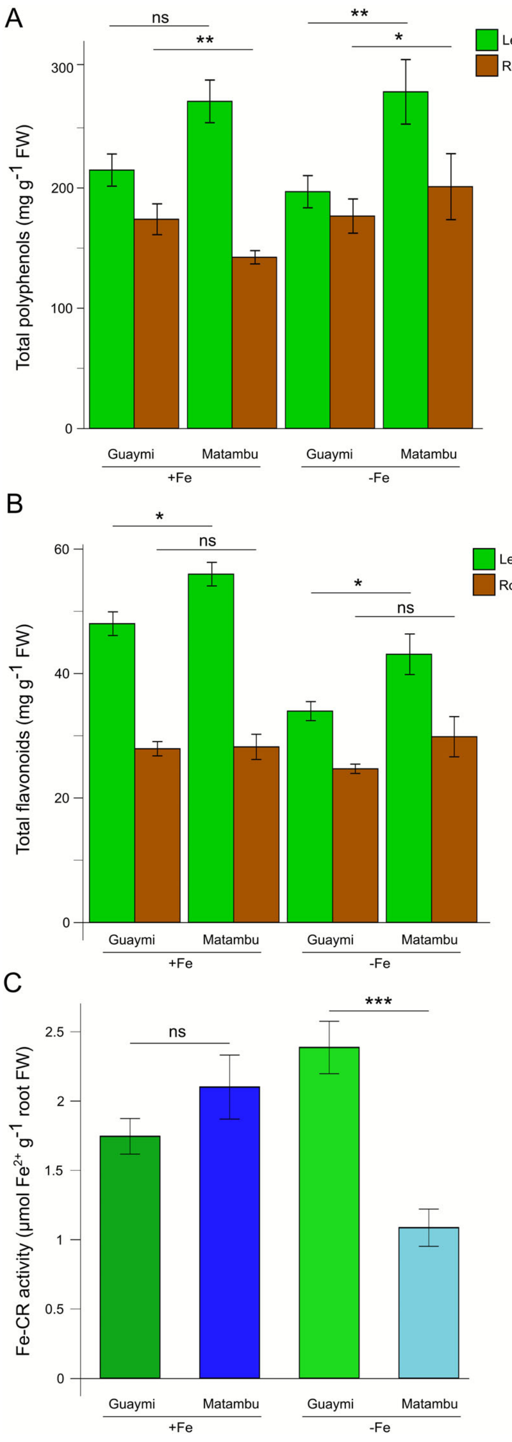

Fig. 4. (A) Total polyphenol and (B) total flavonoid content of leaf and roots (mg g^{-1} FW) and (C) Fe-chelate-reductase (FeCR) activity in roots (μmol Fe^{2+} g^{-1} root FW) of Guaymí (HI) and Matambú (LI) genotypes under sufficient (+Fe, 45 μM FeEDTA) and deficient (−Fe, 0 μM FeEDTA) Fe conditions. Data represent means ± SD for five biological replicates. Differences in total polyphenols between varieties within each compartment (leaf, root) and iron treatment were assessed using independent *t*-tests. Asterisks indicate statistically significant differences between varieties: ns = not significant; * = $P \leq 0.05$; ** = $P \leq 0.01$; *** = $P \leq 0.001$.

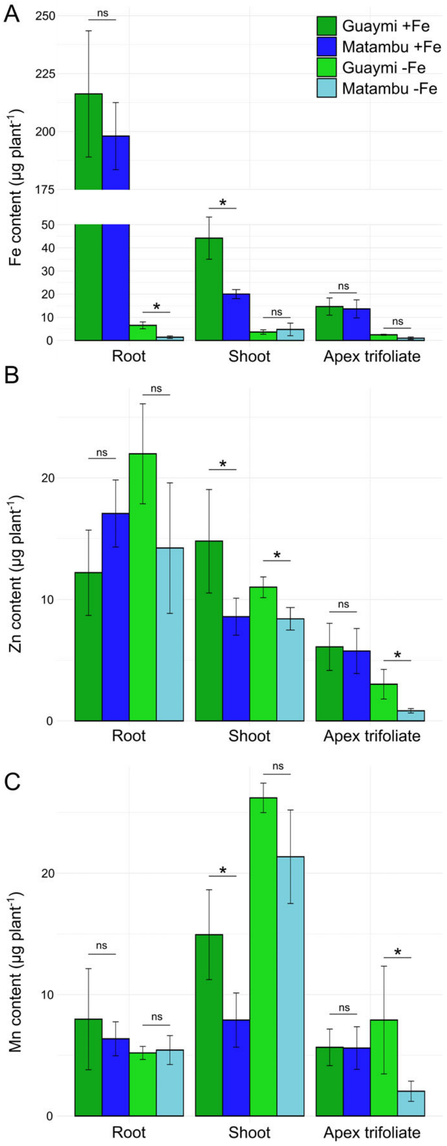

Fig. 5. Micronutrient content (μg plant^{-1}) of (A) Fe, (B) Zn, and (C) Mn in the root, shoot, and the apex trifoliate of Guaymí (HI) and Matambú (LI) genotypes under sufficient (+Fe, 45 μM FeEDTA) and deficient (-Fe, 0 μM FeEDTA) Fe conditions. Data represent means ± SD for five biological replicates. Differences in Fe, Zn, and Mn content between varieties within each compartment (root, shoot, apex trifoliate) and iron treatment were assessed using independent *t*-tests. Asterisks indicate statistically significant differences between varieties: ns = not significant; * = $P \leq 0.05$.

showed a similar transient increase at 4 h and again at 72 h, indicating an intermittent response to iron deficiency in leaf tissues.

DISCUSSION

Screening seeds from 25 different *P. vulgaris* genotypes revealed Fe concentrations ranging from 51.94 to 76.92 mg kg^{-1} DM. Because the seeds were produced in their respective regions,

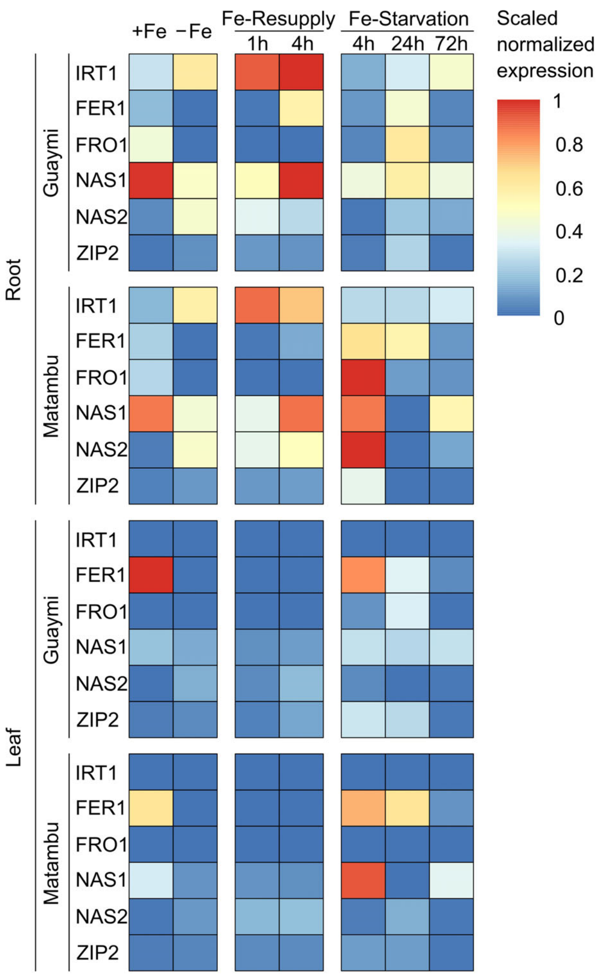

Fig. 6. Heatmap of the scaled normalised expression of iron-dependent genes (IRT1, FER1, FRO1, NAS1, NAS2, ZIP2 in roots and leaves of Guaymí (HI) and Matambú (LI) genotypes grown for 1 week under sufficient (+Fe, 45 μM FeEDTA) and deficient (-Fe, 0 μM FeEDTA) Fe conditions. Additionally, Fe resupply (1 h, 4 h) and Fe deficiency (4 h, 24 h, 72 h) were performed after 1 week of growth. Data are means ± SE of five biological replicates. Normalised gene expression values (relative to reference genes Actin and Tubulin) were filtered, log-transformed using log1p, and scaled via min–max normalisation to highlight relative expression differences across samples for each gene.

environmental effects between locations cannot be fully excluded; however, within each regional group all genotypes were grown under uniform field conditions, allowing reliable comparison among genotypes. The low-Fe genotypes in this screening exhibited Fe levels similar to those in other low-mineral Mesoamerican (e.g., DOR 500, 48.70 mg kg^{-1} DM Fe) and Andean (e.g., CAL96, 46.00 mg kg^{-1} DM Fe) varieties (Beebe 2020). Notably, the low-Fe varieties screened in this study exhibited higher Zn concentrations than LI (12.85 mg kg^{-1} DM Zn), with DOR 500 and CAL96 containing 24.30 and 21.00 mg kg^{-1} DM Zn, respectively. Genotypes exhibiting the highest Fe concentrations, ranging from 74.99 to 76.92 mg kg^{-1} DM Fe, were comparable to high-mineral lines such as SMC 33 (78.00 mg kg^{-1} DM Fe) (Beebe 2020). Zn concentrations, however, were lower in HI (22.70 mg kg^{-1} DM Zn) than in SMC 33 (32.00 mg kg^{-1} DM Zn) (Beebe 2020). In comparison, Graham *et al.* (1999) screened over 1,000 common bean genotypes and reported a wider variation in mineral content, with Fe concentrations ranging from 34 to 89 mg kg^{-1} and Zn concentrations from 21 to 54 mg kg^{-1}. This broader range indicates that the variation observed in the current set of 25 genotypes represents a subset of the total diversity identified in larger germplasm collections. Overall, LI and HI represent ideal choices, offering a clear contrast between a putatively Fe-inefficient variety (LI) and an Fe-efficient variety (HI) for further analysis.

Reduced stunting and chlorosis in HI under iron deficiency

In the current study, the Fe efficiency trait of HI was associated with less growth inhibition and higher chlorophyll content under iron deficiency conditions (Fig. 2A). Previous studies have described the role of Fe in plant growth, photosynthesis, and chlorophyll and carotenoid biosynthesis (Thoiron *et al.* 1997; Rout & Sahoo 2015; Sun *et al.* 2022). It has been found that plants need around 10^{-9} to 10^{-4} M of Fe to alleviate chlorosis and achieve optimal growth (Kim & Guerinot 2007). Similarly, it has been shown that Fe-efficient varieties of common bean (Krouma *et al.* 2003) and soybean (Santos *et al.* 2015) exhibit higher growth and less chlorosis than inefficient varieties. Correspondingly, LI showed growth inhibition and lower SPAD values, which could be attributed to severe chlorosis due to reduced iron availability (Fig. 2B,C). The higher incidence of chlorosis on the apex trifoliate than on the primary leaves is attributed to the immobility of Fe in the plant, which makes it less available in the upper actively growing young organs than in the relatively older parts (Hochmuth 2011; Rout & Sahoo 2015).

The iron efficient bean genotype showed enhanced Fe uptake, mobilisation, and acidification but reduced polyphenol secretion

The current results showed that under iron deficiency the growth medium of the HI bean genotype reached a 14.6% lower pH than that of LI, indicating stronger acidification by HI roots. This decrease in medium pH was observed during daily pH tracking (Fig. 3A), and the difference became more pronounced when proton extrusion was measured in a medium composed of KCl and $CaCl_2$ (Fig. 3B). Such acidification of the growth medium is a typical response of dicotyledonous plants employing Strategy I for iron uptake. These plants release protons, thereby acidifying the rhizosphere and facilitating the reduction of insoluble iron (Ric de Vos *et al.* 1986; Santi & Schmidt 2009). Other studies have reported similar genotypic differences in the ability to acidify the growth medium, depending on iron efficiency status. Three iron deficiency-tolerant common bean cultivars acidified the medium more strongly than sensitive cultivars during daily pH recordings and during 7–8 h incubations in proton extrusion medium (Krouma *et al.* 2003; Slatni *et al.* 2009). Therefore, the higher medium acidification capacity observed for HI is likely associated with its greater Fe efficiency.

In addition to higher acidification, HI showed higher FeCR enzyme activity under iron-deficient conditions. HI reduced 54.4% more Fe than LI under iron deficiency conditions (Fig.

5). Numerous authors have shown that FeCR is strongly induced in roots in response to Fe deficiency in Strategy I plants (Waters *et al*. 2002; Kobayashi & Nishizawa 2012). Similar studies have shown upregulation of FeCR and differences in activity due to genotypical differences under the same Fe deficiency. Root-based FeCR activity was higher under Fe-deficient conditions, and the iron-tolerant genotypes of common beans maintained a higher Fe^{3+} to Fe^{2+} reduction than the inefficient ones (Krouma *et al*. 2003). An efficient bean genotype achieved higher FeCR activity, reduction, and nodulation than inefficient genotypes on its roots (Slatni *et al*. 2009). As the trait of iron uptake efficiency in plants is associated with higher reductase activity under iron deficiency (Moog & Brüggemann 1994; Marschner, 2012), the higher reduction activity of HI observed in this study could confirm its iron uptake efficiency.

The results reported here also indicated that Fe deficiency promoted higher polyphenol production in leaves. This time, LI produced more polyphenols than HI in leaves; LI secreted about 1.4 times more polyphenols than HI in the leaves (Fig. 4A). Similarly, LI maintained higher flavonoid levels in leaves under Fe deficiency. Under iron deficiency conditions, some 'strategy I' plants produce a wide range of molecules collectively termed 'root exudates'. These exudates include organic acids, phenolics, flavins, and flavonoids (Dakora & Phillips 2002; Cesco *et al*. 2010; Abadía *et al*. 2011; Wang *et al*. 2022). Phenolics and flavonoids have both chelating and reducing capacities and form brown complexes with Fe (Mira *et al*. 2002; Grillet & Schmidt 2017; Rajniak *et al*. 2018). Thus, they are thought to contribute to iron reduction in some strategy I plants, although their Fe-reducing capacity is minimal compared with that of the FeCR enzyme (Grusak *et al*. 1990; Rodriguez-Celma *et al*. 2013). Furthermore, iron deficiency-induced root-secreted phenolics have been shown to inhibit root FeCR activity and proton extrusion or acidification in peas (Jin *et al*. 2007). Thus, the high production of polyphenols in roots and shoots in the LI genotype could be a factor in its low FeCR activity, low acidification, and correspondingly low root Fe uptake, and hence its Fe-inefficiency.

Although total seed polyphenol concentrations did not significantly differ between HI and LI (Table 1), previous work in common bean has shown that specific seed polyphenols can either enhance or inhibit Fe bioavailability in mammalian cell models (Hart *et al*. 2017, 2020). While Guaymí and Matambú displayed similar total polyphenol content in the seeds, León-Cortés *et al*. (2025) reported that Guaymí accumulates significantly higher levels of ferulic acid, isoquercetin, and epicatechin-polyphenols potentially relevant to iron homeostasis. Whether such polyphenols also influence Fe uptake and distribution within the plant remains largely unknown. Findings from the current study support the idea that polyphenols and flavonoids play subtle and potentially genotype-specific roles in Fe homeostasis, and further research should aim to dissect the functional impact of individual compounds in plant iron nutrition.

HI partitioned more iron in roots and showed a higher translocation of Fe and Mn in the above-ground parts

For Fe partitioning among the plant organs of the genotypes, content rather than concentration was considered, as differences in organ size could result in smaller organs appearing to have disproportionately higher Fe levels. Results indicated a 6.6-fold higher Fe content in the roots and 1.6-fold higher Fe content in the shoot apex of the iron-starved HI genotype compared with the LI genotype. A higher capacity to deploy an Fe-stressed root response of iron reduction under Fe-limited conditions is a critical feature of iron efficiency among plant genotypes (Marschner, 2012). The Fe reduction response alone correlates with less chlorosis in efficient bean genotypes under iron-limited conditions (Ellsworth *et al*. 1997). Correspondingly, several authors have shown higher root iron content in efficient genotypes under the same conditions. For example, the HI genotype of soybean registered a higher root Fe concentration and a higher Fe content distributed in the apex trifoliate than its LI counterpart under Fe-deficient conditions (Santos *et al*. 2015; Qiu *et al*. 2017). The two critical determinants of a genotype's Fe efficiency are its ability to grow under Fe-limiting conditions and its capacity to deploy a robust root response to facilitate Fe uptake from the soil (García-Mina *et al*. 2013). Given the limited availability of Fe in the environment, it is crucial to allocate any accessible Fe to the root system, which underpins the efficiency discussed herein. The HI genotype showed a higher Fe uptake capacity, accompanied by increased rhizosphere acidification and Fe^{3+} reduction. This capacity could explain its higher root Fe content, reduced growth inhibition, and lower chlorosis under Fe-limited conditions than LI.

In addition, it has been shown that there is a strong relationship between the uptake of Fe and other micronutrients such as Zn and Mn. The functions of these micronutrients are tightly linked; many are redox active and mainly involved in similar roles as metalloproteins and metalloenzymes (Rai *et al*. 2021). Furthermore, plant uptake transporters for Fe, Mn, and Zn were found to be relatively unspecific. For example, IRT1 is a primary root Fe transporter that can also transport Zn and Mn (Vert *et al*. 2002; Grotz & Guerinot 2006). Similarly, cation diffusion facilitator (CDF) transporters, which regulate the efflux of Fe^{2+}, Zn^{2+}, and Mn^{2+} into the cytoplasm or subcellular components, are commonly shared (Gustin *et al*. 2011). They also share a common chelator, nicotianamine (NA) (Connorton *et al*. 2017). Zn, Fe, and Mn are also commonly stored in the provascular bundles and surrounding cell layers in common bean seeds (Cvitanich *et al*. 2011).

In the long term, Zn and Mn are expected to be absorbed at higher levels under iron-deficient conditions, generally in both genotypes, because many Fe-binding ligands and transporters have a high affinity for other divalent metals such as Zn, Mn, or Cu (Kobayashi & Nishizawa 2012). The general increase in Zn and Mn in the HI and LI genotypes under iron deficiency is consistent with the findings of Lešková *et al*. (2017), who observed an enhanced accumulation of Zn, Mn, and other heavy metals in *Arabidopsis* shoots under Fe deficiency. Similarly, Fe deficiency promoted a higher uptake of Zn (337.0%) and Mn (2145.5%) compared with the control plants of *Brassica* (Maillard *et al*. 2016). However, the differences in Zn and Mn uptake between the HI and LI genotypes could be attributed to their contrasting Fe efficiency. Under Fe deficiency, the efficient genotype accumulated higher amounts of Zn and Mn in the uppermost youngest leaves compared with the inefficient genotype. HI accumulated 2.7 and 3.4 times more Zn and Mn, respectively, in the apex trifoliate than LI.

The efficiency of the HI genotype, as evidenced by a high uptake process characterised by high acidification and reduction under Fe deficiency, coupled with sufficient Zn and Mn in the media, may have promoted the uptake of Zn and Mn by HI. In the absence of Fe, HI could have preferentially used its robust Fe uptake process for similar divalent cations (Zn and Mn). In addition, higher Zn and Mn concentrations in the shoot apex of HI could have resulted from less damage from Fe deficiency, as indicated by less growth inhibition and higher chlorophyll content. Alternatively, the HI genotype may exhibit a higher translocation rate, although this cannot be fully determined from the present study.

Sustained iron uptake in HI vs. transient response in LI

The differential expression patterns of iron-responsive genes in the root and leaf tissues of the two bean genotypes, HI and LI, under varying iron conditions were highly consistent with the different physiology (Fig. 6). These findings indicate that root tissues in both genotypes were more responsive to iron fluctuations than leaves, reflecting the essential role of roots in sensing and adapting to nutrient availability (Hantzis *et al.* 2018). Additionally, the contrasting responses of HI and LI, particularly under Fe resupply and deficiency, revealed genotype-specific regulatory mechanisms in iron homeostasis.

Under Fe-sufficient conditions, both genotypes exhibited low expression of iron-responsive genes, suggesting a minimal need for active iron uptake or redistribution in iron-rich environments. This baseline expression is consistent with studies in other plant species, where iron homeostasis genes have low activity under sufficient conditions, likely because of tightly regulated feedback mechanisms that prevent excess iron uptake and toxicity (Nabila & Guerinot 2021). The elevated expression of *NAS1* and *FRO1* in HI under sufficient conditions suggests a preparatory or basal role in iron mobilisation, indicating a slightly more proactive iron management approach than LI.

Upon prolonged Fe deficiency, both genotypes showed similar upregulation of *IRT1, NAS1*, and *NAS2* in the roots, suggesting a conserved response to low-iron availability. This upregulation aligns with the known roles of IRT1 in iron uptake and *NAS* genes in iron mobilisation within plant tissues (Vert *et al.* 2002; Klatte *et al.* 2009). However, the marked divergence in expression patterns upon Fe resupply highlights the notable transient differences in genotype-specific Fe recovery mechanisms. In HI, the rapid and sustained increase in *IRT1*, *NAS1*, and *NAS2*, along with the delayed upregulation of *FER1*, suggests a swift and robust adaptation to reintroduced iron, which is consistent with physiological data. This scenario likely reflects an efficient iron acquisition and storage strategy, where HI prioritises rapid iron uptake and allocation to ferritin (FER1) for storage, a pattern observed in other iron efficient genotypes (Slatni *et al.* 2009; Waters *et al.* 2018). In contrast, LI's more moderate response, with lower *IRT1, NAS1*, and *NAS2* increases, suggests a less vigorous approach to iron resupply, potentially indicative of a more conservative iron uptake strategy or lower sensitivity to resupplied iron.

Under Fe deficiency at 4, 24, and 72 h, HI and LI exhibited distinct expression dynamics, confirming differing adaptive strategies. HI slowly upregulated *IRT1* and consistently elevated *NAS1* levels. This response indicates prolonged adaptation to iron scarcity, enabling HI to maximise iron acquisition over extended periods of deprivation. The delayed but transient peaks in *FRO1* and *FER1* at 24 h further suggest that HI is not only attempting to acquire iron through *IRT1* but also mobilising and storing any available iron efficiently. In contrast, LI's transient response, characterised by an initial spike in *FER1, FRO1, NAS1, NAS2*, and *ZIP2* at 4 h followed by a rapid decline, points to a short-term adaptation (or the more severe transient Fe deficiency in that genotype). This response may reflect a strategy where LI responds acutely to iron deficiency but lacks the prolonged upregulation of iron transport genes such as *IRT1*, possibly leading to a less sustained iron acquisition capability under prolonged deficiency, consistent with the different performance with Fe deficiency.

Leaf tissues in both genotypes showed markedly lower expression of iron-responsive genes than roots, suggesting that leaves play a secondary role in iron sensing/remobilisation and homeostasis. The predominant upregulation of *FER1* in both genotypes under Fe sufficiency and deficiency highlights the primary function of ferritin in storing and managing iron to prevent oxidative stress in leaves (Ravet *et al.* 2009; Parveen *et al.* 2016). This observation is consistent with previous studies where the role of ferritin in leaves was primarily protective, buffering iron fluctuations while avoiding cellular damage (Ravet *et al.* 2009). The upregulation of *NAS1* by HI across all deficiency points and the transient *NAS1* response of LI suggest limited but genotype-specific attempts to mobilise iron within leaves during deprivation. However, the subdued expression changes in both genotypes under prolonged deficiency indicate a limited iron-responsive signalling capacity in leaves. This leaf-based low inhibition supports the idea that leaves rely on root-driven iron acquisition and are less involved in compensatory iron uptake during deficiency (Bienfait *et al.* 1987; Wu *et al.* 2012). Furthermore, it is possible that similarities or differences in gene expression are not well represented in the proteome; therefore, genotype-specific differences in the abundance, stability, and functionality of iron-regulated proteins are also possible.

This study highlights distinct iron regulatory mechanisms in bean genotypes under iron-deficient conditions, emphasising the superiority of the iron efficient (HI) genotype. The HI genotype demonstrated enhanced iron uptake through a synergistic interaction between apoplastic acidification and FeCR activity. This results in increased iron reduction, improved iron uptake efficiency, and overall resilience in low-iron environments. This response contrasts with the iron-inefficient (LI) genotype, which relies more on polyphenol release, a strategy that is less effective for mobilising iron and maintaining consistent iron uptake. The robust iron uptake mechanism of HI appears to enhance the uptake of iron and other essential divalent cations, increasing Zn and Mn levels in young shoot tissues, and potentially contributing to its better performance under iron-deficient conditions. Additionally, the genotypical transcriptional differences in iron deficiency sensing and response, characterised by HI's stable, progressive response compared with LI's erratic reaction, shed light on the importance of the time dependence of iron regulation for iron deficiency tolerance. It should be noted, however, that the conclusions regarding Fe efficiency in this study are based on a comparison of only a single HI genotype and a single LI genotype. Including additional well-characterised HI and LI genotypes in future studies would be advantageous to assess the generality and universality of the observed regulatory mechanisms in common beans. The 25 genotypes initially analysed in this study were adapted to different geographical regions and agroecological contexts. Although variation in seed Fe concentration has been reported among common bean genotypes, previous studies have also indicated that, although there is evidence of genotypic stability in Fe-related traits among environments (Mutari *et al.* 2022), an influence by environmental conditions and genotype × environment interactions can also be found (Katuuramu *et al.* 2021). Thus, the differences observed among genotypes may reflect both the intrinsic physiological characteristics and environmental modulation of Fe accumulation in the seeds. In the present study, contrasting phenotypes provided a useful framework for examining genotype-dependent responses to Fe deficiency under controlled conditions.

Taken together, the contrasting iron uptake and regulatory strategies of HI and LI highlight genotypic variation that could be leveraged in breeding programmes to develop bean varieties with enhanced iron efficiency and improved resilience in iron-limited soils. Insights into the sustained iron regulatory response of HI offer a promising genetic basis for improving iron use efficiency and minimising growth inhibition due to iron deficiency. These findings deepen the understanding of iron homeostasis and support breeding strategies aimed at micronutrient biofortification and improved mineral nutrition in legumes and other crops. By integrating these findings, we can advance toward developing bean genotypes that not only thrive in iron-limited conditions but also contribute to addressing micronutrient deficiencies in human diets.

AUTHOR CONTRIBUTIONS

All authors contributed to the conception and design of the study as well as the interpretation of the data. FXR and NJM performed the included experiments, conducted data analysis, and drafted the manuscript. AH-P conducted data analysis, provided critical revisions, and contributed to the final version of the manuscript. UL and IC provided critical revisions and contributed to the final version of the manuscript.

ACKNOWLEDGEMENTS

We would like to thank all members of the Department of Nutritional Crop Physiology at the University of Hohenheim who were involved in this study for their valuable support. Special thanks to J.S., A.K., and H.O. for their assistance throughout the study. Open Access funding enabled and organized by Projekt DEAL.

FUNDING INFORMATION

This research was supported by the German Academic Exchange Service (DAAD) under the funding programme ID: 57552340. Publishing fees supported by Funding Programme Open Access Publishing of University of Hohenheim.

DATA AVAILABILITY STATEMENT

Data supporting the findings of this study are available from the corresponding author upon reasonable request.

SUPPORTING INFORMATION

Additional supporting information may be found online in the Supporting Information section at the end of the article.

Table S1. List of genes and their primer sequences.

REFERENCES

Abadía J., Vázquez S., Rellán-Álvarez R., El-Jendoubi H., Abadía A., Álvarez-Fernández A., López-Millán A.F. (2011) Towards a knowledge-based correction of iron chlorosis. *Plant Physiology and Biochemistry*, **49**, 471–482.

Ainsworth E.A., Gillespie K.M. (2007) Estimating total phenolic content and other oxidation substrates in plant tissues using Folin-Ciocalteu reagent. *Nature Protocols*, **2**, 875–877.

Beebe S. (2020) Biofortification of common bean for higher iron concentration. *Frontiers in Sustainable Food Systems*, **4**, 573449.

Beebe S., Gonzalez A.V., Rengifo J. (2000) Research on trace minerals in the common bean. *Food and Nutrition Bulletin*, **21**, 387–391.

Bereczky Z., Wang H.-Y., Schubert V., Ganal M., Bauer P. (2003) Differential regulation of nramp and irt metal transporter genes in wild type and iron uptake mutants of tomato. *Journal of Biological Chemistry*, **278**, 24697–24704.

Bienfait H.F., De Weger L.A., Kramer D. (1987) Control of the development of iron-efficiency reactions in potato as a response to iron deficiency is located in the roots. *Plant Physiology*, **83**, 244–247.

Bouis H.E., Saltzman A. (2017) Improving nutrition through biofortification: A review of evidence from HarvestPlus, 2003 through 2016. *Global Food Security*, **12**, 49–58.

Bravo-Monzón A.E., Montiel-González C., Benítez-Malvido J., Arena-Ortíz M.L., Flores-Puerto J.I., Chiappa-Carrara X., Avila-Cabadilla L.D., Alvarez-Añorve M.Y. (2022) The assembly of tropical dry forest tree communities in anthropogenic landscape: The role of chemical defense. *Plants*, **11**, 516.

Broadley M., Brown P., Cakmak I., Rengel Z., Zhao F. (2012) Chapter 7 - function of nutrients: Micronutrients. In: Marschner P. (Ed), *Marschner's mineral nutrition of higher plants*, 3rd edition. Academic Press, London, pp 191–248.

Broughton W.J., Hernández G., Blair M., Beebe S., Gepts P., Vanderleyden J. (2003) Beans (*Phaseolus* spp.) – Model food legumes. *Plant and Soil*, **252**, 55–128.

Brown J.C. (1972) Competition between phosphate and the plant for Fe from Fe^{2+} ferrozine. *Agronomy Journal*, **64**, 240–243.

Cesco S., Neumann G., Tomasi N., Pinton R., Weisskopf L. (2010) Release of plant-borne flavonoids into the rhizosphere and their role in plant nutrition. *Plant and Soil*, **329**, 1–25.

Chaney R.L., Brown J.C., Tiffin L.O. (1972) Obligatory reduction of ferric chelates in iron uptake by soybeans. *Plant Physiology*, **50**, 208–213.

Connolly E.L., Campbell N.H., Grotz N., Prichard C.L., Guerinot M.L. (2003) Overexpression of the *FRO2* ferric chelate reductase confers tolerance to growth on low iron and uncovers posttranscriptional control. *Plant Physiology*, **133**, 1102–1110.

Connorton J.M., Balk J., Rodríguez-Celma J. (2017) Iron homeostasis in plants – A brief overview. *Metallomics*, **9**, 813–823.

Cvitanich C., Przybyłowicz W.J., Mesjasz-Przybyłowicz J., Blair M.W., Astudillo C., Orłowska E., Jurkiewicz A.M., Jensen E.Ø., Stougaard J. (2011) Micro-PIXE investigation of bean seeds to assist micronutrient biofortification. *Nuclear Instruments and Methods in Physics Research Section B: Beam Interactions with Materials and Atoms*, **269**, 2297–2302.

Dakora F.D., Phillips D.A. (2002) Root exudates as mediators of mineral acquisition in low-nutrient environments. In: Adu-Gyamfi J.J. (Ed), *Food security in nutrient-stressed environments: Exploiting plants' genetic capabilities*. Springer Netherlands, Dordrecht, pp 201–213.

de Vos C.R., Lubberding H.J., Bienfait H.F. (1986) Rhizosphere acidification as a response to iron deficiency in bean plants. *Plant Physiology*, **81**(3), 842–846.

Durrett T.P., Gassmann W., Rogers E.E. (2007) The FRD3-mediated efflux of citrate into the root vasculature is necessary for efficient iron translocation. *Plant Physiology*, **144**, 197–205.

Ellsworth J.W., Jolley V.D., Nuland D.S., Blaylock A.D. (1997) Screening for resistance to iron deficiency chlorosis in dry bean using iron reduction capacity. *Journal of Plant Nutrition*, **20**, 1489–1502.

FAO (1999) Phaseolus bean: Post-harvest operations, *LIPhO Post-Harvest Compendium*. Food and

Agriculture Organization, Rome https://www.fao.org/3/a-av015e.pdf

FAO (2015) World reference base for soil resources 2014 (update 2015), *World Soil Resources Reports 106*. Food and Agriculture Organization of the United Nations, Rome http://www.fao.org/3/i3794en/I3794en.pdf

Gambino G., Perrone I., Gribaudo I. (2008) A rapid and effective method for RNA extraction from different tissues of Grapevine and other woody plants. *Phytochemical Analysis*, **19**(6), 520–525.

García-Mina J.M., Bacaicoa E., Fuentes M., Casanova E. (2013) Fine regulation of leaf iron use efficiency and iron root uptake under limited iron bioavailability. *Plant Science*, **198**, 39–45.

Ghandilyan A., Vreugdenhil D., Aarts M.G.M. (2006) Progress in the genetic understanding of plant iron and zinc nutrition. *Physiologia Plantarum*, **126**, 407–417.

Glahn R.P., Noh H. (2021) Redefining bean iron biofortification: A review of the evidence for moving to a high Fe bioavailability approach. *Frontiers in Sustainable Food Systems*, **5**, 682130.

Glahn R.P., Tako E., Cichy K., Wiesinger J. (2016) The cotyledon cell wall and intracellular matrix are factors that limit iron bioavailability of the common bean (*Phaseolus vulgaris*). *Food & Function*, **7**, 3193–3200.

Graham R., Senadhira D., Beebe S., Iglesias C., Monasterio I. (1999) Breeding for micronutrient density in edible portions of staple food crops: Conventional approaches. *Field Crops Research*, **60**, 57–80.

Grillet L., Schmidt W. (2017) The multiple facets of root iron reduction. *Journal of Experimental Botany*, **68**, 5021–5027.

Grotz N., Guerinot M.L. (2006) Molecular aspects of Cu, Fe and Zn homeostasis in plants. *Biochimica et Biophysica Acta (BBA) - Molecular Cell Research*, **1763**, 595–608.

Grusak M.A., Welch R.M., Kochian L.V. (1990) Does iron deficiency in *Pisum sativum* enhance the activity of the root plasmalemma iron transport protein? *Plant Physiology*, **94**, 1353–1357.

Gustin J.L., Zanis M.J., Salt D.E. (2011) Structure and evolution of the plant cation diffusion facilitator family of ion transporters. *BMC Evolutionary Biology*, **11**, 76.

Hantzis L.J., Kroh G.E., Jahn C.E., Cantrell M., Peers G., Pilon M., Ravet K. (2018) A program for iron economy during deficiency targets specific Fe proteins. *Plant Physiology*, **176**(1), 596–610.

Hart J.J., Tako E., Glahn R.P. (2017) Characterization of polyphenol effects on inhibition and promotion of iron uptake by Caco-2 cells. *Journal of Agricultural and Food Chemistry*, **65**, 3285–3294.

Hart J.J., Tako E., Wiesinger J., Glahn R.P. (2020) Polyphenolic profiles of yellow bean seed coats and their relationship with iron bioavailability. *Journal of Agricultural and Food Chemistry*, **68**, 769–778.

Hochmuth G. (2011) *Iron (Fe) Nutrition of Plants*. EDIS. https://edis.ifas.ufl.edu

Hoppler M., Zeder C., Walczyk T. (2009) Quantification of ferritin-bound iron in plant samples by isotope tagging and species-specific isotope dilution mass spectrometry. *Analytical Chemistry*, **81**, 7368–7372.

Jin C.W., You G.Y., He Y.F., Tang C., Wu P., Zheng S.J. (2007) Iron deficiency-induced secretion of phenolics facilitates the reutilization of root apoplastic iron in red clover. *Plant Physiology*, **144**, 278–285.

Katuuramu D.N., Wiesinger J.A., Luyima G.B., Nkalubo S.T., Glahn R.P., Cichy K.A. (2021) Investigation of genotype by environment interactions for seed zinc and iron concentration and iron bioavailability in common bean. *Frontiers in Plant Science*, **12**, 670965.

Kim S.A., Guerinot M.L. (2007) Mining iron: Iron uptake and transport in plants. *FEBS Letters*, **581**, 2273–2280.

King K.E., Peiffer G.A., Reddy M., Lauter N., Lin S.F., Cianzio S., Shoemaker R.C. (2013) Mapping of iron and zinc quantitative trait loci in soybean for association to iron deficiency chlorosis resistance. *Journal of Plant Nutrition*, **36**, 2132–2153.

Klatte M., Schuler M., Wirtz M., Fink-Straube C., Hell R., Bauer P. (2009) The analysis of *Arabidopsis* nicotianamine synthase mutants reveal functions for nicotianamine in seed iron loading and iron deficiency responses. *Plant Physiology*, **150**, 257–271.

Kobayashi T., Nishizawa N.K. (2012) Iron uptake, translocation, and regulation in higher plants. *Annual Review of Plant Biology*, **63**, 131–152.

Krouma A., Gharsalli M., Abdelly C. (2003) Differences in response to iron deficiency among some lines of common bean. *Journal of Plant Nutrition*, **26**, 2295–2305.

León-Cortés D., Arce-Villalobos K., Bogantes-Ledezma D., Irías-Mata A., Chaves-Barrantes N., Vinas M. (2025) Anti-aflatoxin potential of phenolic compounds from common beans (*Phaseolus vulgaris L.*). *Food Chemistry*, **469**, 142597.

Lešková A., Giehl R.F.H., Hartmann A., Fargašová A., von Wirén N. (2017) Heavy metals induce iron deficiency responses at different hierarchic and regulatory levels. *Plant Physiology*, **174**, 1648–1668.

Lin Y.-F., Liang H.-M., Yang S.-Y., Boch A., Clemens S., Chen C.-C., Wu J.F., Huang J.L., Yeh K.C. (2009) *Arabidopsis* IRT3 is a zinc-regulated and plasma membrane localized zinc/iron transporter. *New Phytologist*, **182**, 392–404.

Maillard A., Etienne P., Diquélou S., Trouverie J., Billard V., Yvin J.-C., Ourry A. (2016) Nutrient deficiencies modify the ionomic composition of plant tissues: A focus on crosstalk between molybdenum and other nutrients in *Brassica napus*. *Exbot Journal*, **67**, 5631–5641.

Marschner H. (2012) *Marschner's mineral nutrition of higher plants*, Vol. **89**. Academic Press, London, pp 651.

Mira L., Tereza Fernandez M., Santos M., Rocha R., Helena Florêncio M., Jennings K.R. (2002) Interactions of flavonoids with iron and copper ions: A mechanism for their antioxidant activity. *Free Radical Research*, **36**, 1199–1208.

Moog P.R., Brüggemann W. (1994) Iron reductase systems on the plant plasma membrane—A review. *Plant and Soil*, **165**, 241–260.

Moraghan J.T., Padilla J., Etchevers J.D., Grafton K., Acosta-Gallegos J.A. (2002) Iron accumulation in seed of common bean. *Plant and Soil*, **246**, 175–183.

Murray M.G., Thompson W.F. (1980) Rapid isolation of high molecular weight plant DNA. *Nucleic Acids Research*, **8**(19), 4321–4325.

Mutari B., Sibiya J., Gasura E., Kondwakwenda A., Matova P.M., Chirwa R. (2022) Genotype × environment interaction and stability analyses of grain yield and micronutrient (Fe and Zn) concentrations in navy bean (*Phaseolus vulgaris* L.) genotypes under varied production environments. *Field Crops Research*, **286**, 108607.

Nabila R., Guerinot M.L. (2021) All together now: Regulation of the iron deficiency response. *Journal of Experimental Botany*, **6**, 2045–2055.

Parveen S., Gupta D.B., Dass S., Kumar A., Pandey A., Chakraborty S., Chakraborty N. (2016) Chickpea ferritin CaFer1 participates in oxidative stress response and promotes growth and development. *Scientific Reports*, **6**, 31218.

Passarelli S., Free C.M., Shepon A., Beal T., Batis C., Golden C.D. (2024) Global estimation of dietary micronutrient inadequacies: A modelling analysis. *The Lancet Global Health*, **12**, e1590–e1599.

Petry N., Boy E., Wirth J.P., Hurrell R.F. (2015) Review: The potential of the common bean (*Phaseolus vulgaris*) as a vehicle for iron biofortification. *Nutrients*, **7**, 1144–1173.

Pinheiro C., Baeta J.P., Pereira A.M., Domingues H., Ricardo C.P. (2010) Diversity of seed mineral composition of *Phaseolus vulgaris* L. germplasm. *Journal of Food Composition and Analysis*, **23**, 319–325.

Qiu W., Dai J., Wang N., Guo X., Zhang X., Zuo Y. (2017) Effects of Fe-deficient conditions on Fe uptake and utilization in P-efficient soybean. *Plant Physiology and Biochemistry*, **112**, 1–8.

Rai S., Singh P.K., Mankotia S., Swain J., Satbhai S.B. (2021) Iron homeostasis in plants and its crosstalk with copper, zinc, and manganese. *Plant Stress*, **1**, 100008.

Rajniak J., Giehl R.F.H., Chang E., Murgia I., von Wirén N., Sattely E.S. (2018) Biosynthesis of redox-active metabolites in response to iron deficiency in plants. *Nature Chemical Biology*, **14**, 442–450.

Ravet K., Touraine B., Boucherez J., Briat J.-F., Gaymard F., Cellier F. (2009) Ferritins control interaction between iron homeostasis and oxidative stress in *Arabidopsis*. *The Plant Journal*, **57**, 400–412.

Rawal V.N. (2019) *The global economy of pulses*. FAO, Rome, Italy.

Ritchie H., Roser M. (2019) Micronutrient deficiency. Published online OurWorldInData.org. https://ourworldindata.org/micronutrient-deficiency

Robinson N.J., Procter C.M., Connolly E.L., Guerinot M.L. (1999) A ferric-chelate reductase for iron uptake from soils. *Nature*, **397**, 694–697.

Rodriguez-Celma J., Lin W.-D., Fu G.-M., Abadia J., Lopez-Millan A.-F., Schmidt W. (2013) Mutually exclusive alterations in secondary metabolism are critical for the uptake of insoluble iron compounds by *Arabidopsis* and *Medicago truncatula*. *Plant Physiology*, **162**, 1473–1485.

Rodríguez-Lucena P., Ropero E., Hernández-Apaolaza L., Lucena J.J. (2010) Iron supply to soybean plants through the foliar application of IDHA/Fe^{3+}: Effect of plant nutritional status and adjuvants. *Journal of the Science of Food and Agriculture*, **90**, 2633–2640.

Römheld V., Marschner H. (1986) Evidence for a specific uptake system for iron phytosiderophores in roots of grasses. *Plant Physiology*, **80**, 175–180.

Roschzttardtz H., Conéjéro G., Divol F., Alcon C., Verdeil J.-L., Curie C., Mari S. (2013) New insights into Fe localization in plant tissues. *Frontiers in Plant Science*, **4**, 350.

Rout G.R., Sahoo S. (2015) Role of iron in plant growth and metabolism. *RAS*, **3**, 1–24.

Santi S., Schmidt W. (2009) Dissecting iron deficiency-induced proton extrusion in *Arabidopsis* roots. *New Phytologist*, **183**, 1072–1084.

Santos C.S., Roriz M., Carvalho S.M.P., Vasconcelos M.W. (2015) Iron partitioning at an early growth stage impacts iron deficiency responses in soybean plants (*Glycine max* L.). *Frontiers in Plant Science*, **6**, 325.

Schuler M., Rellán-Álvarez R., Fink-Straube C., Abadía J., Bauer P. (2012) Nicotianamine functions in the phloem-based transport of iron to sink organs, in pollen development and pollen tube growth in *Arabidopsis*. *The Plant Cell*, **24**, 2380–2400.

Schulte E.E. (2004) A3554 Soil and applied iron. Understanding plant nutrients. Cooperative Extension Publications. University of Wisconsin-Extension, RP 08-2004 (I09/92).

Shukla A.K., Behera S.K., Prakash C., Tripathi A., Patra A.K., Dwivedi B.S., Trivedi V., Rao C.S., Chaudhari S.K., das S., Singh A.K. (2021) Deficiency of phyto-available sulphur, zinc, boron, iron, copper and manganese in soils of India. *Scientific Reports*, **11**, 19760.

Singh G., Ambreen H., Jain P., Chakraborty A., Singh B., Manivannan A., Bhatia S. (2023a) Comparative transcriptomic and metabolite profiling reveals genotype-specific responses to Fe starvation in chickpea. *Physiologia Plantarum*, **175**, e13897.

Singh S., Singh A.L., Pal K.K., Reddy K.K., Gangadhara K., Dey R., Mahatma M.K., Verma A., Kumar N., Patel C.B., Thawait L.K., Ahmed S., Navapara R., Rani K., Kona P. (2023b) Accumulation of resveratrol, ferulic acid and iron in seeds confer iron deficiency chlorosis tolerance to a novel genetic stock of peanut (Arachis hypogaea L.) grown in calcareous soils. *Physiology and Molecular Biology of Plants*, **29**, 725–737.

Slatni T., Krouma A., Gouia H., Abdelly C. (2009) Importance of ferric chelate reductase activity and acidification capacity in root nodules of N_2-fixing common bean (*Phaseolus vulgaris* L.) subjected to iron deficiency. *Symbiosis*, **47**, 35–42.

Stevens G.A., Beal T., Mbuya M.N.N., Luo H., Neufeld L.M., Addo O.Y., Adu-Afarwuah S., Alayón S., Bhutta Z., Brown K.H., Jefferds M.E., Engle-Stone R., Fawzi W., Hess S.Y., Johnston R., Katz J., Krasevec J., McDonald C.M., Mei Z., Osendarp S., Paciorek C.J., Petry N., Pfeiffer C.M., Ramirez-Luzuriaga M.J., Rogers L.M., Rohner F., Sethi V., Suchdev P.S., Tessema M., Villapando S., Wieringa F.T., Williams A.M., Woldeyahannes M., Young M.F. (2022) Micronutrient deficiencies among preschool-aged children and women of reproductive age worldwide: A pooled analysis of individual-level data from population-representative surveys. *The Lancet Global Health*, **10**, e1590–e1599.

Sun Y., Luo J., Feng P., Yang F., Liu Y., Liang J., Wang H., Zou Y., Ma F., Zhao T. (2022) MbHY5-MbYSL7 mediates chlorophyll synthesis and iron transport under iron deficiency in *Malus baccata*. *Frontiers in Plant Science*, **13**, 1035233.

Thoiron S., Pascal N., Briat J.-F. (1997) Impact of iron deficiency and iron resupply during the early stages of vegetative development in maize (*Zea mays* L.). *Plant, Cell & Environment*, **20**, 1051–1060.

Urwat U., Ahmad S.M., Masi A., Ganai N.A., Murtaza I., Khan I., Zargar S.M. (2021) Fe and Zn stress-induced gene expression analysis unraveled mechanisms of mineral homeostasis in common bean (*Phaseolus vulgaris* L.). *Scientific Reports*, **11**, 24026.

Vasconcelos M., Eckert H., Arahana V., Graef G., Grusak M.A., Clemente T. (2006) Molecular and phenotypic characterization of transgenic soybean expressing the *Arabidopsis* ferric chelate reductase gene, *FRO2*. *Planta*, **224**, 1116–1128.

Vert G., Grotz N., Dédaldéchamp F., Gaymard F., Guerinot M.L., Briat J.-F., Curie C. (2002) IRT1, an *Arabidopsis* transporter essential for iron uptake from the soil and for plant growth. *The Plant Cell*, **14**, 1223–1233.

von Wirén N., Klair S., Bansal S., Briat J.-F., Khodr H., Shioiri T., Leigh R.A., Hider R.C. (1999) Nicotianamine chelates both FeIII and FeII. Implications for metal transport in plants. *Plant Physiology*, **119**, 1107–1114.

Wang B., Wei H., Chen Z., Li Y., Zhang W.-H. (2022) Carbonate-induced chemical reductants are responsible for iron acquisition in strategy I wild herbaceous plants native to calcareous grasslands. *Plant and Cell Physiology*, **63**, 770–784.

Waters B.M., Amundsen K., Graef G. (2018) Gene expression profiling of iron deficiency chlorosis sensitive and tolerant soybean indicates key roles for phenylpropanoids under alkalinity stress. *Frontiers in Plant Science*, **9**, 10.

Waters B.M., Blevins D.G., Eide D.J. (2002) Characterization of *FRO1*, a pea ferric-chelate reductase involved in root iron acquisition. *Plant Physiology*, **129**, 85–94.

Welch R.M., Graham R.D. (2004) Breeding for micronutrients in staple food crops from a human nutrition perspective. *Journal of Experimental Botany*, **55**, 353–364.

Wiersma J.V. (2005) High rates of Fe-EDDHA and seed iron concentration suggest partial solutions to iron deficiency in soybean. *Agronomy Journal*, **97**, 924–934.

Wiersma J.V. (2012) Is seed iron concentration predictive of resistance to iron deficiency in soybean? *Crop Science*, **52**, 471–481.

Wu T., Zhang H.-T., Wang Y., Jia W.-S., Xu X.-F., Zhang X.-Z., Han Z.H. (2012) Induction of root Fe(III) reductase activity and proton extrusion by iron deficiency is mediated by auxin-based systemic signaling in *Malus xiaojinensis*. *Journal of Experimental Botany*, **63**, 859–870.